



Treatment of Terasil Red R Dye Wastewater using H_2O_2 /pyridine/Cu(II) System

Chooi Ling Lim, Norhashimah Morad*, Tjoon Tow Teng, Norli Ismail

School of Industrial Technology, Universiti Sains Malaysia, 11800 Penang, Malaysia

ARTICLE INFO

Article history:

Received 12 June 2008

Received in revised form 8 January 2009

Accepted 9 February 2009

Available online 21 February 2009

Keywords:

CCD

COD

Decolorization

Factorial Design

H_2O_2 /pyridine/Cu(II)

Sludge

ABSTRACT

The H_2O_2 /pyridine/Cu(II) advanced oxidation system was used to assess the efficiency of the treatment of a 1 g L^{-1} Terasil Red R dye solution. This system was found to be capable in reducing the concentration of chemical oxygen demand (COD) of the dye solution up to 90%, and achieving 99% in decolorization at the optimal concentration of $5.5\text{ mM } H_2O_2$, 38 mM pyridine and 1.68 mM Cu(II). The final concentration of COD was recorded at 117 mg L^{-1} and color point at 320 PtCo. Full 2^4 factorial design and the response surface methodology using central composite design (CCD) were utilized in the screening and optimization of this study. Treatment efficiency was found to be pH independent. The amount of sludge generation was in the range of $100\text{--}175\text{ mg L}^{-1}$ and the sludge produced at the optimal concentration was 170 mg L^{-1} .

© 2009 Elsevier B.V. All rights reserved.

1. Introduction

Dyes are widely used in the textile, printing, leather, food, cosmetics and paper industries. These substances are customarily left in the industrial wastes and subsequently discharged to the surface water resources [1]. Dyeing wastewater are strongly colored, and contain high amounts of suspended solids, broad fluctuating pH, surfactants and high chemical oxygen demand (COD) which is deemed unacceptable under most country's environmental regulations [2–4]. Hence, great emphasis has been placed in the research on the treatment of this contaminated effluent.

Currently, there are various technologies available in the treatment of dye wastewater. Among them are adsorption, ion-exchange, Fenton oxidation, ozonation, coagulation and precipitation, cucurbituril, aerobic and anaerobic processes, and membrane filtration [5]. The negative aspects of these technologies are that either they lack the efficiency in reducing the many diverse pollutants in the dye wastewater or when the treatment technology appears to be promising, the cost of operation is very high thus prohibiting the particular technology to be applied to the large scale wastewater, common to the above industries. Therefore, by optimizing the operating factors using statistical design of experiment, a more feasible and economical method in achieving good treatment results could be offered.

Advanced Oxidation Processes (AOPs) are another promising treatment method in treating biorefractory compounds [6]. The use of H_2O_2 , a universal, ecologically clean and strong oxidant in another series of AOP involving a combination of a transition metal ion with ligand molecules in the decomposition of H_2O_2 to produce hydroxyl radicals (OH^*) in the H_2O_2 /pyridine/Cu(II) oxidation treatment system was studied on the decolorization of various synthetic dyes [7–10]. The attractiveness of this system is that apart from yielding the decolorization efficiency of over 90% for most dyes, decolorization using this system can be carried out unaffected by pH in the range of 3–9 [7]. Based on this information, this study was carried out to investigate further, the capability of this system in the treatment of a synthetic disperse dye wastewater, especially in the reduction of COD since there was no information on COD reduction using this system. In this paper, comparisons of spectra obtained from Fourier Transform Infrared (FT-IR) spectroscopy between the original dye powder and the oxidized dye residue were made. FT-IR was used to identify the structural changes of the molecules in detail wherein different compounds have their own FT-IR spectra and therefore, unique molecular fingerprints can be identified [11].

Conventional treatment technologies such as the coagulation process often produce high amount of sludge at the end of the treatment which requires further treatment [12]. Therefore, the aims of the research work were to determine the effectiveness of this system in the reduction of COD, the removal of color, as well as to compare the amount of sludge produced at the end of this treatment with other treatment systems. In addition, FT-IR analysis was conducted to determine the structural changes of the original dye and the oxidized dye residues.

* Corresponding author. Tel.: +60 4 6532236; fax: +60 4 6573678.
E-mail address: nhashima@usm.my (N. Morad).

Table 1
General properties of Terasil Red R (1 g L⁻¹).

Parameter	Terasil Red R
Color Index (CI) name	CI Disperse Red 324
Class	Disperse
λ_{\max} (nm)	470
pH	5.9 ^a
COD (mg L ⁻¹)	1172 ^a
Color Point (PtCo)	32150 ^a

^a Average value of 20 samples for dye solution with concentration 1 g L⁻¹.

2. Experiments

2.1. Chemicals

Terasil Red R (CI Disperse Red 324), a commercial disperse dye powder was procured from CIBA and was directly used as received without further purification. Properties of Terasil Red R were given in Table 1. The λ_{\max} was measured using a UV–visible spectrophotometer (Shimadzu UV-1601PC). H₂O₂ (35%) was obtained from R&M chemicals, pyridine (analytical grade) was obtained from Merck, and CuSO₄·5H₂O, NaOH and H₂SO₄ were obtained from System ChemAR. Distilled water was used for the preparation of all dye solutions, stock solutions, and dilution of acid and base in this work.

2.2. Methods

All experiments were performed in a standard jar-test apparatus (Velp Scientifica JLT 6) comprising of six stirring rods. Six 500 mL beakers, each filled with 150 mL dye solution, fixed at the initial dye concentration of 1 g L⁻¹ were used in each run. The desired pH was adjusted using 0.1 M NaOH and 0.1 M H₂SO₄ before the addition of H₂O₂, pyridine and CuSO₄·5H₂O. pH was measured using a pH meter (CyberScan 20).

Mixing time and mixing speed were fixed at 6 min and 60 rpm, respectively. Reaction time was kept constant at 60 min and all samples were filtered using Whatman No. 4 filter paper (pore size 20–25 μ m). Filtered samples were then sent for the measurement of COD and color point. FT-IR spectra of Terasil Red R dye powder and the sludge were recorded on a FT-IR spectrometer (PerkinElmer 2000) over the range of 4000–400 cm⁻¹ using the KBr disc technique.

Degradation products of Terasil Red R were analyzed using gas chromatography–mass spectrometry (GC–MS). 50 mL of samples was subjected to liquid–liquid extraction and the organic extracts were evaporated to dryness. A Hewlett Packard 6890 gas chromatograph (GC) with 5973N mass selective (MS) detector and chemstation data system was used. The capillary column used was HP-5 crosslinked 5% phenyl methyl siloxane fused silica with film thickness of 30 m \times 0.25 mm \times 0.25 μ m. Initial temperature was programmed at 70 °C, rising at 20 °C/min to 280 °C. Helium was used as the carrier gas. Identifications of dye degradation products were based on mass spectral matched with standard compounds stored in NIST and Wiley libraries.

COD was determined using the closed reflux, colorimetric method according to procedures in *Standard Methods*, Method No. 5220D. Samples were placed in ampules followed by the addition of COD digestion solution and inverted several times to ensure complete mixing before being placed in a COD reactor (HACH) which was preheated to 150 °C. Samples were kept refluxed for 2 h. After 2 h, samples were left to cool to room temperature before the measurement of COD absorption at 620 nm wavelength by a spectrophotometer (HACH DR/2010) was conducted. The digested distilled water sample was used as the blank reference solution and the difference between the absorbance of a digested blank sample

and the digested sample was the COD measurement of the sample [13].

Color point measurement is reported as true color according to the spectrophotometric—single wavelength method using DR 2010 HACH spectrophotometer adopted from *Standard Methods*, Method No. 2120C, in which the true color of samples and platinum cobalt standards follows Beer's Law. Distilled water was filled in a spectrophotometer cell and was used to zero the instrument. Cells were then filled with samples and absorbance measurement at 455 nm was recorded as the true color of samples [13].

Sludge production was determined by Total Suspended Solids (TSS) dried at 103–105 °C according to *Standard Methods*, Method No. 2540D. Pre-prepared glass fiber filter paper (Whatman GF-C filter paper, pore size 1.2 μ m) was filled with a small volume of distilled water. While stirring the sample, a measured volume was pipetted onto the seated glass fiber filter in crucibles. Samples were then dried for 1 h at 103 °C in an oven. The amount of sludge produced is calculated as follows [13]:

$$\text{mg total suspended solids, L} = \frac{(A - B) \times 1000}{\text{sample volume, mL}} \quad (1)$$

where *A* is the weight of crucible + dried residue (mg) and *B* is the weight of the crucible (mg).

2.3. Statistical Design of Experiments

2.3.1. Full Factorial Design

The 2^k factorial design was utilized in this study in order to determine the joint effects of several factors on a response. This design provides the smallest number of treatment combinations with which *k* factors can be studied in a complete factorial arrangement. The advantage of using factorial design is that this design allows effects of a factor to be estimated at several levels of other factors giving valid conclusions over a wide range of experimental conditions. Without the use of this design, important interactions among factors may not be detected and thus, leads to misleading conclusions [14].

In this study, pH, [H₂O₂], [pyridine], and [Cu(II)] were chosen as independent factors and the percentage of COD reduction as the main dependent factor response. Other variables such as mixing time and speed were fixed at 6 min and 60 rpm, respectively.

2.3.2. Central Composite Design (CCD)

Response Surface Methodology (RSM) is a technique used in modeling and analysis of problems in which a response of interest is influenced by several factors and the objective is to optimize this response. Response surface is normally represented graphically where the contour plot are often drawn to visualize the shape of the response surface. In the contour plot, lines of constant response are drawn where each contour corresponds to a particular height of the response surface [14]. The first step in RSM is to find a suitable approximation for the true functional relationship between the yield of the process, *y* and the set of independent factors either by the first-order model or the second-order model. When a process is relatively close to the optimum, the second-order model that incorporates curvature is usually required to approximate the response [14]:

$$Y = \beta_0 + \sum_{i=1}^k \beta_i x_i + \sum_{i=1}^k \beta_{ii} x_i^2 + \sum_{i=1}^{k-1} \sum_{j=2}^k \beta_{ij} x_i x_j \quad (2)$$

where *Y* is the predicted response, β_0 the offset term, β_i the linear effect, β_{ii} the squared effect and β_{ij} represents the interaction effect. After performing the screening of factors with the factorial design, a response surface analysis was employed to optimize the

highest COD reduction of a Terasil Red R dye solution. Coded variables were converted to natural variables according to the following relationship [14]:

$$x_k = \frac{\xi_k - x_0}{\delta x} \quad (3)$$

where x_k is the coded value of the k th independent variable, ξ_k the natural variable of the k th independent variable, x_0 the natural value of the k th independent variable at the center point, and δx is the value of step change.

2.4. Analyses

Results of the experimental designs were analyzed using Minitab 14 (PA, USA) statistical software to estimate the response of dependent response variable and to obtain the effects, coefficients, standard deviation of coefficients as well as other statistical parameters of the model. Optimized condition was obtained from contour plot graphically and also by solving the polynomial regression equation. Quality of fit was expressed by coefficient of determination R^2 and statistical significance was analyzed in Analysis of Variance (ANOVA) in which the level of significance at 5% probability level was given as values of P less than 0.05 [15].

3. Results and discussion

3.1. Screening of independent factors for percentage COD reduction

In this study, the independent factors screened consisted of pH, $[H_2O_2]$, [pyridine], and [Cu(II)]. The influence of factors was determined by measuring the percentage of COD reduction.

Effects of factors and their interactions were determined by performing the experiment according to Table 2 in triplicate with 3 blocks, each block containing 2 center points to obtain the standard error of the coefficients as well as to detect a curvature of

Table 2

The input factors of H_2O_2 /pyridine/Cu(II) System and experimental ranges and levels of 2^4 Full Factorial Design.

Experiment	Block	Experimental factors			
		A pH	B H_2O_2 (mM)	C pyridine (mM)	D Cu(II) (mM)
1	1	4	7	50	1.5
2	1	4	7	30	1.5
3	1	6	6	40	1.6
4	1	4	7	30	1.7
5	1	4	5	30	1.5
6	1	4	5	50	1.5
7	1	8	7	50	1.5
8	1	6	6	40	1.6
9	1	4	5	30	1.7
10	1	4	7	50	1.7
11	1	8	5	50	1.7
12	1	8	7	50	1.7
13	1	8	7	30	1.7
14	1	8	5	30	1.7
15	1	8	7	30	1.5
16	1	8	5	50	1.5
17	1	4	5	50	1.7
18	1	8	5	30	1.5

Factors	Levels	
	–(Low level)	+(High level)
A: (pH)	4	8
B: ($[H_2O_2]$)	5 mM	7 mM
C: ([pyridine])	30 mM	50 mM
D: ([Cu(II)])	1.5 mM	1.7 mM

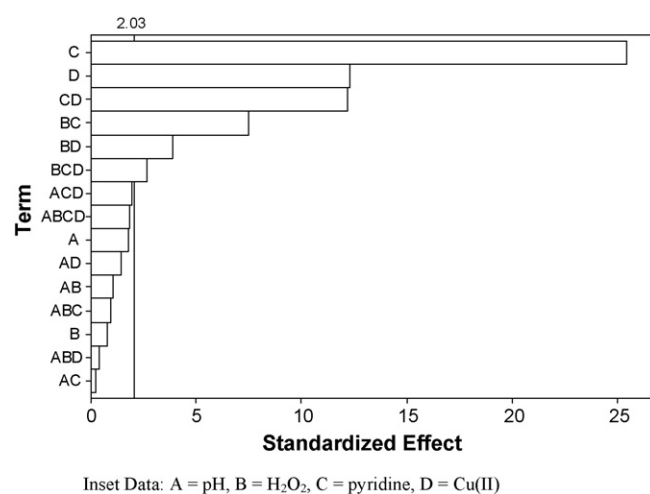


Fig. 1. Pareto chart of the standardized effect for % COD reduction.

the system forming the 2^4 full factorial design. Factor levels were coded as –(low level) and +(high level). Low level is the level where the lowest concentration of chemicals was used and high level is the level where the highest concentration of chemicals was used [16].

The Pareto chart of standardized effects at $P=0.05$ is presented in Fig. 1 in order to better evaluate the effect of each factor and the interactions among the factors, where any values with an absolute value higher than 2.03 are considered significant. Fig. 1 shows that factor A (pH) is not significant, and all interactions involving factor A are negligible. Therefore, factor A was discarded from this study.

Above pH 8, only a few transition metal complexes can catalyze oxidation by H_2O_2 . Precipitation occurred when Cu(II) and H_2O_2 were used in alkaline conditions. However, the presence of pyridine can stabilize metal ions in basic solution and thus prevents precipitation [8]. Due to this reason, the complete H_2O_2 /pyridine/Cu(II) system can be carried out in a wide range of pH. Further experiments were performed using the initial pH of the dye solution without any pH adjustments.

3.2. Optimization of percentage COD reduction

Central Composite Response Surface Design was used to obtain the relationship between the factors and response and to optimize the response. A full 2^3 factorial design plus 4 center points in cube, 6 axial points and 2 center points in axial as presented in Table 3 was carried out in three replicates and six blocks in order to fit the second-order polynomial model.

Range and levels of the factors were arrived based on the earlier screening results which indicated the presence of a curvature which meant that the experimental ranges were relatively close to the optimum. The quadratic regression model for the percentage COD reduction in terms of coded factors regardless of their significance is given in the following equation:

$$Y = 89.0115 - 0.0056x_1 - 0.7034x_2 + 0.8948x_3 - 0.0445x_1^2 - 0.5895x_2^2 - 0.5820x_3^2 - 0.3154x_1x_2 - 0.1204x_1x_3 + 0.4646x_2x_3 \quad (4)$$

where Y is the predicted response, x_1 , x_2 and x_3 are the coded values of the respective treatment system factors; H_2O_2 , pyridine and Cu(II).

It is necessary to check the fitted model to ensure adequate approximation to the actual system. Therefore, the diagnostic plot such as the predicted versus actual values plot was used in order to

Table 3

The input factors of H₂O₂/pyridine/Cu(II) System in coded and natural variables and experimental ranges and levels of process variables for % COD reduction.

Experiment	Block	Experimental factors					
		Coded variables			Natural variables		
		B	C	D	B (mM)	C (mM)	D (mM)
1	1	+1	+1	-1	7	50	1.5
2	1	-1	+1	-1	5	50	1.5
3	1	0	0	0	6	40	1.6
4	1	+1	-1	+1	7	30	1.7
5	1	0	0	0	6	40	1.6
6	1	0	0	0	6	40	1.6
7	1	+1	+1	+1	7	50	1.7
8	1	0	0	0	6	40	1.6
9	1	-1	+1	+1	5	50	1.7
10	1	-1	-1	+1	5	50	1.7
11	1	+1	-1	-1	7	30	1.5
12	1	-1	-1	-1	5	30	1.5
13	2	0	0	0	6	40	1.6
14	2	0	-α	0	6	24	1.6
15	2	+α	0	0	7.6	40	1.6
16	2	0	0	+α	6	40	1.76
17	2	0	0	-α	6	40	1.44
18	2	0	+α	0	6	56	1.6
19	2	0	0	0	6	40	1.6
20	2	-α	0	0	4.4	40	1.6

Factors	Levels				
	-α	-1	0	+1	+α
B: [H ₂ O ₂]	4.4 mM	5 mM	6 mM	7 mM	7.6 mM
C: [pyridine]	24 mM	30 mM	40 mM	50 mM	56 mM
D: [Cu(II)]	1.44 mM	1.5 mM	1.6 mM	1.7 mM	1.76 mM

judge the adequacy of the model [17]. The predicted versus actual values plot for percentage COD reduction is presented in Fig. 2 and the value of R^2 is 0.9774 showing a satisfactory prediction of the experimental data.

In order to examine the effects of factors towards the response, a graphical representation known as the contour plots of the model from Eq. (4) were used and are presented in Fig. 3. Contour plots in Fig. 3 show that the maximum COD reduction 88.9% was achieved at level of H₂O₂ between -1 and 0 (concentration between 5 mM and 6 mM), level of pyridine between -1 and 0 (concentration between 30 mM and 50 mM), and level of Cu(II) between 0 and +1 (concentration between 1.6 mM and 1.7 mM).

In order to locate the levels of x_1, x_2, \dots, x_k that optimize the predicted response known as stationary point, a mathematical solution of second-order model in matrix notation is written as [14]:

$$\hat{y} = \hat{\beta}_0 + x'b + x'Bx \quad (5)$$

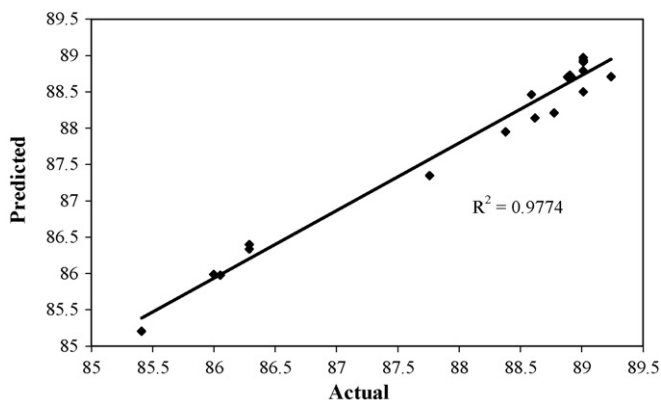


Fig. 2. Predicted versus actual value for % COD reduction.

Contour Plots of % COD reduction

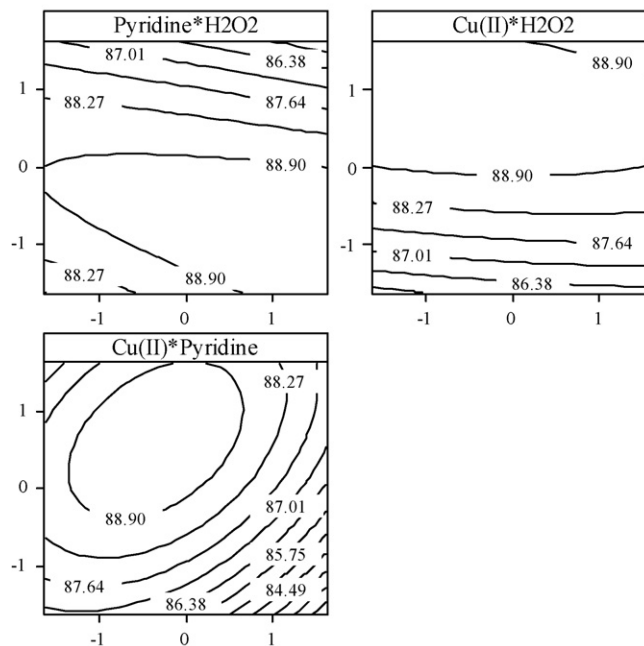


Fig. 3. Contour plots of % COD reduction.

where

$$x = \begin{bmatrix} x_1 \\ x_2 \\ \vdots \\ x_k \end{bmatrix}, \quad b = \begin{bmatrix} \hat{\beta}_1 \\ \hat{\beta}_2 \\ \vdots \\ \hat{\beta}_k \end{bmatrix}, \quad B = \begin{pmatrix} \hat{\beta}_{11} & \hat{\beta}_{12}/2 & \hat{\beta}_{1k}/2 \\ \hat{\beta}_{12}/2 & \hat{\beta}_{22} & \hat{\beta}_{2k}/2 \\ \hat{\beta}_{13}/2 & \hat{\beta}_{23}/2 & \hat{\beta}_{33} \end{pmatrix} \quad (6)$$

The derivative of \hat{y} with respect to the elements of vector x equals 0:

$$\frac{\partial \hat{y}}{\partial x} = b + 2Bx = 0 \quad (7)$$

From Eq. (5), the stationary point is:

$$x_s = -\frac{1}{2}B^{-1}b \quad (8)$$

By substituting Eq. (6) into Eq. (5), the predicted response at stationary point is:

$$\hat{y}_s = \hat{\beta}_0 + \frac{1}{2}x_s'b \quad (9)$$

The stationary point was located by solving Eq. (8), where:

$$b = \begin{bmatrix} -0.0056 \\ -0.7034 \\ 0.8948 \end{bmatrix}, \quad B = \begin{pmatrix} -0.0445 & -0.1577 & -0.0602 \\ -0.1577 & -0.5895 & 0.2323 \\ -0.0602 & 0.2323 & -0.5820 \end{pmatrix}$$

$$\therefore x_s = \begin{bmatrix} -0.5053 \\ -0.1637 \\ 0.7557 \end{bmatrix}$$

In terms of natural variables, the stationary point was converted according to Eq. (3) in order to obtain ξ_1, ξ_2 and ξ_3 representing [H₂O₂], [pyridine], and [Cu(II)], respectively.

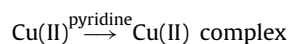
After having solved Eq. (3), [H₂O₂], [pyridine], and [Cu(II)] were found to be at 5.5 mM, 38 mM, and 1.68 mM, respectively. These values were very close to the stationary point found by visual observation of the contour plots in Fig. 3.

From Eq. (9), the predicted response at the stationary point could be obtained and the predicted response was calculated as

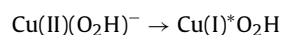
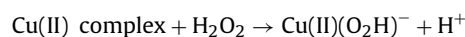
$\hat{y}_s = 89.41\%$. The observed experimental value performed by using concentrations at the stationary point was found to be 89.97% which was very close with the predicted value.

3.3. The H_2O_2 /pyridine/Cu(II) system

H_2O_2 /pyridine/Cu(II) system uses a chelating ligand and a transition metal, forming a transition metal complex to produce superoxide anions (*O_2) and hydroxyl radicals (OH^*), which then function in the degradation of wide ranges of polycyclic aromatic hydrocarbons [7,18]. Pyridine coordinates copper to form cupric complex [18,19]:



Cupric complex with H_2O_2 is reduced to cuprous complex [18,19]:



Cuprous complex will then react with excess H_2O_2 to generate reactive radicals such as *O_2 and OH^* [18,19].



3.3.1. Effects of H_2O_2 , pyridine, and Cu(II) towards treatment efficiency

In this H_2O_2 /pyridine/Cu(II) system, H_2O_2 acts as the oxidant, pyridine as the ligand and Cu(II) acts as the catalyst [10]. Oxidation of the aromatic substrates ensues along with decomposition of H_2O_2 in the production of OH^* in the presence of pyridine in which the OH^* is responsible in the degradation of the dye [20].

All AOPs were reported to be capable in decolorizing dye wastewater within 30 min of reaction time [9]. Attention was placed on the reduction of COD in this study because COD measures the content of organic matter in a sample. Even though with high decolorization efficiency (above 90%), the structured dye molecules are oxidized into smaller organic molecules such as acetic acids, aldehydes, ketones, etc., instead of CO_2 and H_2O where these molecules contribute significantly to the concentration of COD [21]. Therefore, the measurement of color alone is insufficient to draw conclusion on the efficiency of a treatment in reducing the level of pollution of a sample.

Having obtained the optimum concentrations for H_2O_2 , pyridine, and Cu(II), the following experiments were carried out to investigate the individual effects of $[H_2O_2]$, $[pyridine]$, and $[Cu(II)]$ towards treatment efficiency in terms of COD reduction and decolorization.

3.3.2. Effect of $[H_2O_2]$

In this set of experiment, the $[pyridine]$ and $[Cu(II)]$ were kept constant at their respective optimal concentrations; 38 mM pyridine and 1.68 mM Cu(II), while $[H_2O_2]$ was varied from 0 mM to 25 mM. The effect of $[H_2O_2]$ towards treatment efficiency is presented in Fig. 4(a).

COD reduction increased with $[H_2O_2]$, from 46% to 89% until 5 mM where further increase in the concentration led to decrease in COD reduction 84%. This was due to inhibition caused by high $[H_2O_2]$. At high $[H_2O_2]$, the following reactions were significant [22]:

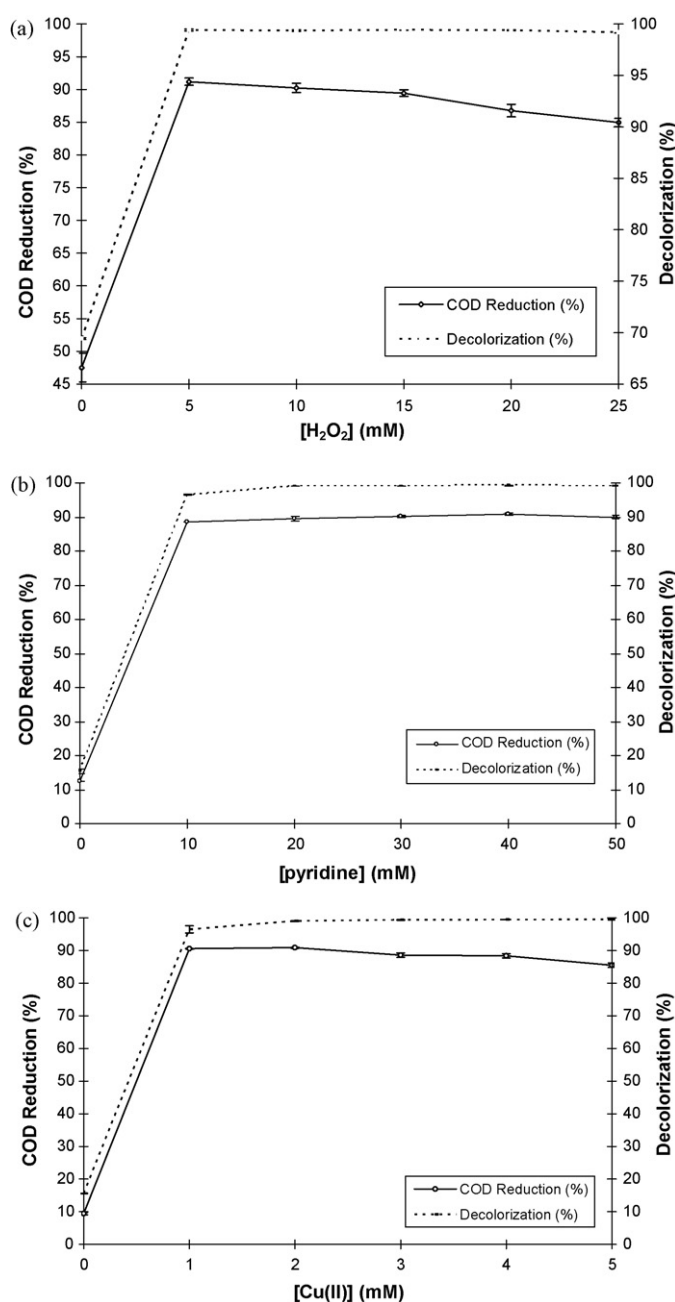
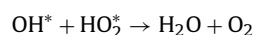
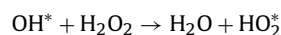


Fig. 4. Effect of [factors] towards treatment efficiency; (a) $[H_2O_2]$, (b) $[pyridine]$ (c) $[Cu(II)]$.

The over dosage of H_2O_2 led to the scavenging effect of this substance on free radicals, pre-dominating the production effect which eventually increased the concentration of COD and thus, reducing the percentage of COD reduction [23].

Decolorization efficiency increased from 69% to 99% with $[H_2O_2]$ from 0 mM to 5 mM and Fig. 4(a) shows slight fluctuation in percentage of decolorization with further increase in $[H_2O_2]$.

3.3.3. Effect of $[pyridine]$

The effect of $[pyridine]$ was studied by keeping $[H_2O_2]$ and $[Cu(II)]$ constant at their respective optimal concentrations; 5.5 mM H_2O_2 and 1.68 mM Cu(II), while $[pyridine]$ was varied from 0 mM to 50 mM. The effect of $[pyridine]$ towards treatment efficiency in terms of percentage of COD reduction and decolorization is presented in Fig. 4(b).

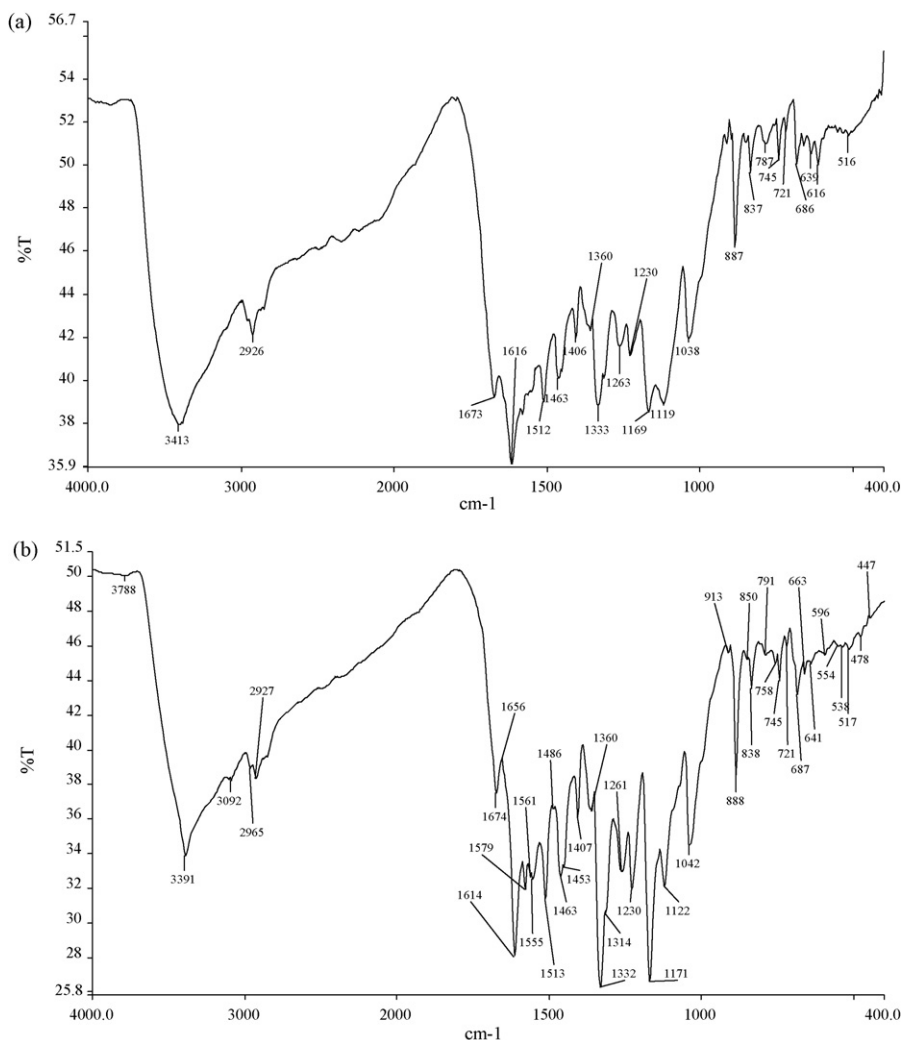


Fig. 5. FT-IR spectra of: (a) Terasil Red R and (b) sludge after H_2O_2 /pyridine/ $\text{Cu}(\text{II})$ oxidation.

COD reduction increased from 11% to 88% and decolorization from 15% to 95% with [pyridine] from 0 mM to 10 mM, respectively. Pyridine plays a role in producing OH^* radicals after forming a complex with $\text{Cu}(\text{II})$ [24]. This explained the reason behind the addition of pyridine which significantly enhanced the COD reduction and decolorization of Terasil Red R.

3.3.4. Effect of $[\text{Cu}(\text{II})]$

The effect of $[\text{Cu}(\text{II})]$ was studied by keeping $[\text{H}_2\text{O}_2]$ and [pyridine] constant at their respective optimal concentrations; 5.5 mM H_2O_2 and 38 mM pyridine while $[\text{Cu}(\text{II})]$ was varied from 0 mM to 5 mM. The effect of $[\text{Cu}(\text{II})]$ towards treatment efficiency in terms of percentage COD reduction and decolorization is presented in Fig. 4(c).

An increase in $[\text{Cu}(\text{II})]$ from 0 mM to 1 mM increased the percentage COD reduction from 9% to 90% and decolorization from 15% to 95%. Increase in $[\text{Cu}(\text{II})]$ after 2 mM enhanced decolorization to 99% while the COD reduction dropped to 85%.

3.3.5. FT-IR spectra of Terasil Red R and oxidized sludge

The FT-IR spectrum of original Terasil Red R dye powder is shown in Fig. 5(a) and the spectra of the oxidized sludge in Fig. 5(b). From Fig. 5(a), among the functional groups observed from the peaks include primary amines group with NH stretch at band 3413 cm^{-1} , alkyl groups (2926 cm^{-1}), amine hydrohalides group

(2352 cm^{-1}), broad and very strong carbonyl ($\text{C}=\text{O}$) stretch at 1798 cm^{-1} , aromatic compounds (1672 cm^{-1}), medium carboxylic acid (1406 cm^{-1}), strong $-\text{C}-\text{O}-\text{C}-$ esters (1038 cm^{-1}), very strong nitro groups (1333 cm^{-1}), medium nitro groups with $\text{C}-\text{N}$ stretch (914 cm^{-1}), and strong $\text{C}-\text{Cl}$ stretch (516 cm^{-1}).

Among the peaks of interest observed in Fig. 5(b) of the oxidized sludge include OH groups (3391 cm^{-1}), aromatic groups (3092 cm^{-1}), strong $-\text{CH}_2-$ (2965 cm^{-1}), very strong carbonyl compounds ($\text{C}=\text{O}$) (1674 cm^{-1}), strong pyridines (1614 cm^{-1}), very strong aliphatic nitro compounds (1579 cm^{-1}), very strong secondary amides (1561 cm^{-1}), broad carboxylic acid salts (1360 cm^{-1}), very strong esters, $-\text{C}-\text{O}-\text{C}-$ (1261 cm^{-1}), strong primary aliphatic amines, $-\text{C}-\text{NH}_2-$ (1042 cm^{-1}), very strong $-\text{CH}=\text{CH}_2-$ (913 cm^{-1}), very strong benzenes (758 cm^{-1}), and strong $\text{C}-\text{Cl}$ stretch (538 cm^{-1}).

3.3.6. Oxidative degradation products of Terasil Red R

Degradation products of Terasil Red R using H_2O_2 /pyridine/ $\text{Cu}(\text{II})$ system was identified using GC-MS. Compounds identified in acidic extraction include 2,4,7,9-tetramethyl-5-dicyne-4,7-diol at a retention time of 6.1 min, propanoic acid, 2-methyl-1-[1,1-dimethylethyl]-2-methyl-1,3-propanediyl ester (7.87 min), benzenamine, 2-chloro-4-nitro (9.44 min), methyl tetradecanoate (9.68 min), 1,2-benzenedicarboxylic acid, bis[2-methyl propyl ester] (12.31 min), hexadecanoic acid, 1-methyl ethyl ester

(15.97 min), 1,3-hexyloxacyclotridec-10-en-2-one (16.61 min), 1-octadecene (17.37 min), 9,12-octadecadienoic acid methyl ester (17.58 min), methyl ricinoleate (22.51 min), eicosanoic acid methyl ester (23.38 min), cholesta-3,5-dien-7-one (30.06 min), and stigmasta-5,22-dien-3-ol (33.62 min).

Compounds identified in basic extraction include hexanedioic acid, dimethyl ester at retention time of 5.33 min, 2,4,7,9-tetramethyl-5-dicyne-4,7-diol (6.13 min), and 1,4-benzenediamine, 2-chloro (6.5 min).

3.4. Sludge production

Total Suspended Solids is used in the measurement of sludge production. The amount of TSS in the treated dye solution measured in this study varied within the range of 100–175 mg L⁻¹. Sludge produced using this treatment was comparatively lower than those from the Fenton treatment which produced sludge within the range of 129–546 mg L⁻¹, and from coagulation using FeCl₃ (326–530 mg L⁻¹) and coagulation using FeSO₄ (61.6–266 mg L⁻¹) [25]. At the optimum concentrations 5.5 mM H₂O₂, 38 mM pyridine and 1.68 mM Cu(II), the amount of sludge produced was 170 mg L⁻¹.

At the end of the treatment, we observed that the color of the sludge (mainly oxidized dye residues) was slightly different from the color of the original dye powder. This could be due to the changes in the functional groups of the original dye powder and the oxidized materials as shown in the results obtained from the FT-IR spectra. Lin and Lai reported in their paper that the slight difference between the colors of the settled sludge with the original dye powder was due to the alteration to the OH functional group of the original dye powder [26].

In Malaysia, sludge disposal is performed by licensed agents. These agents will carry out characterization analysis of the wastes prior to disposal, in order to advice customers on the disposal costs and determine the most appropriate disposal method. Overall treatment costs includes wastes disposal cost at the end of treatment processes and cost required during the operation of treatment processes. Lower amount of sludge produced would generally meant lower costs for disposal.

4. Conclusion

The application of experimental design in the treatment of 1 g L⁻¹ Terasil Red R dye solution using H₂O₂/pyridine/Cu(II) system was applied in evaluating the effect of factors: pH, [H₂O₂], [pyridine], and [Cu(II)] that could affect the response. pH was found to be not an important factor. Optimization by the response surface methodology using CCD was utilized to obtain the optimum [H₂O₂], [pyridine], and [Cu(II)] that resulted in the highest response. The optimal concentrations resulting in the highest COD reduction of 90% were recorded at 5.5 mM of H₂O₂, 38 mM of pyridine, and 1.68 mM of Cu(II). This treatment system recorded 99% decolorization at the optimal concentrations of H₂O₂, pyridine and Cu(II) and the amount of sludge produced was fairly acceptable which was within the range of 100–175 mg L⁻¹.

Acknowledgment

The authors wish to express their sincere appreciation to Universiti Sains Malaysia for providing the Short Term Grant (Grant No.: 304/PTEKIND/638091) for financial support of this study.

References

- [1] G. Muthuraman, T.T. Teng, C.P. Leh, I. Norli, Extraction and recovery of methylene blue from industrial wastewater using benzoic acid as an extractant, *J. Hazard. Mater.* 163 (2009) 363–369.
- [2] T.H. Kim, C. Park, J. Lee, E.B. Shin, S. Kim, Pilot scale treatment of textile wastewater by combined process (fluidized biofilm process-chemical coagulation-electrochemical oxidation), *Water Res.* 36 (2002) 3979–3988.
- [3] B.H. Tan, T.T. Teng, A.K. Mohd Omar, Removal of dyes and industrial dye wastes by magnesium chloride, *Water Res.* 34 (2) (2000) 597–601.
- [4] T.H. Kim, C. Park, J. Yang, S. Kim, Comparison of disperse and reactive dye removals by chemical coagulation and Fenton oxidation, *J. Hazard. Mater.* 112 (B) (2004) 95–103.
- [5] Y. Anjaneyulu, N.S. Chary, S.S.D. Raj, Decolorization of industrial effluents—available methods and emerging technologies—a review, *Environ. Sci. Biotechnol.* 4 (2005) 245–273.
- [6] A.L. Teel, C.R. Warberg, D.A. Atkinson, R.J. Watts, Comparison of mineral and soluble iron Fenton's catalysts for the treatment of trichloroethylene, *Water Res.* 35 (4) (2001) 977–984.
- [7] F. Nerud, P. Baldrian, J. Gabriel, D. Ogbeifun, Decolorization of synthetic dyes by the Fenton reagent and the Cu/pyridine/H₂O₂ system, *Chemosphere* 44 (2001) 957–961.
- [8] P. Verma, P. Baldrian, J. Gabriel, T. Trnka, F. Nerud, Copper–ligand complex for the decolorization of synthetic dyes, *Chemosphere* 57 (2004) 1207–1211.
- [9] U. Bali, B. Karagözoğlu, Performance comparison of Fenton process, ferric coagulation and H₂O₂/pyridine/Cu(II) system for decolorization of Remazol-Turquoise Blue G-133, *Dyes Pigments* 74 (2007) 73–80.
- [10] U. Bali, B. Karagözoğlu, Decolorization of Remazol-Turquoise Blue G-133 and other dyes by Cu/pyridine/H₂O₂ system, *Dyes Pigments* 73 (2007) 133–140.
- [11] G. Sebnem, A.C. Gozen, F. Severcan, Use of Fourier transform infrared spectroscopy for rapid comparative analysis of *Bacillus* and *Micrococcus* isolates, *Food Chem.* 113 (2009) 1301–1307.
- [12] K. Pradeep, B. Prasad, I.M. Mishra, C. Shri, Decolorization and COD reduction of dyeing wastewater from a cotton textile mill using thermolysis and coagulation, *J. Hazard. Mater.* 153 (2008) 635–645.
- [13] Standard Methods, Standard Methods for the Examination of Water and Wastewater, 21st ed. American Public Health Association, Washington, DC: American Public Health Association/American Water Works Association/Water Environment Federation; 2005.
- [14] D.C. Montgomery, Design and Analysis of Experiments, 5th ed., John Wiley & Sons, New York, 2001.
- [15] K. Ravikumar, S.H. Kim, Y.A. Son, Design of experiments for the optimization and statistical analysis of Berberine finishing of polyamide substrates, *Dyes Pigments* 75 (2007) 401–407.
- [16] K. Tanja, Y.M. Slokar, M. Alenka, L. Marechal, B.V. Darinka, The use of experimental design for the evaluation of the influence of variables on the H₂O₂/UV treatment of model textile wastewater, *Dyes Pigments* 58 (2003) 171–178.
- [17] A.L. Ahmad, S.S. Wong, T.T. Teng, A. Zuhairi, Optimization of coagulation-flocculation process for pulp and paper mill effluent by response surface methodological analysis, *J. Hazard. Mater.* 145 (2007) 162–168.
- [18] T. Watanabe, K. Koller, K. Messner, Copper-dependent depolymerization of lignin in the presence of fungal metabolite, pyridine, *J. Biotechnol.* 62 (1998) 221–230.
- [19] L. Pecci, G. Montefoschi, D. Cavallini, Some new details of the copper–hydrogen peroxide interaction, *Biochem. Biophys. Res. Commun.* 235 (1997) 264–267.
- [20] N.I. Kuznetsova, N.V. Kirillova, L.I. Kuznetsova, M.Y. Smirnova, V.A. Likholobov, Hydrogen peroxide and oxygen–hydrogen oxidation of aromatic compounds in catalytic systems containing heteropoly compounds, *J. Hazard. Mater.* 146 (2007) 569–576.
- [21] S.H. Lin, C.M. Lin, Treatment of textile waste effluents by ozonation and chemical coagulation, *Water Res.* 27 (12) (1993) 1743–1748.
- [22] E.C. Catalkaya, F. Kargi, Effects of operating parameters on advanced oxidation of diuron by the Fenton's reagent: a statistical design approach, *Chemosphere* 69 (2007) 485–492.
- [23] O. Gimeno, M. Carbajo, M.J. López, J.A. Melero, F. Beltrán, F.J. Rivas, Photocatalytic promoted oxidation of phenolic mixtures: an insight into the operating and mechanistic aspects, *Water Res.* 41 (2007) 4672–4684.
- [24] P. Verma, V. Shah, P. Baldrian, J. Gabriel, P. Stopka, T. Trnka, F. Nerud, Decolorization of synthetic dyes using a copper complex with glucaric acid, *Chemosphere* 54 (2004) 291–295.
- [25] R. Liu, H.M. Chiu, C.S. Shiau, Y.L. Ruth Yeh, Y.T. Hung, Degradation and sludge production of textile dyes by Fenton and photo-Fenton processes, *Dyes Pigments* 73 (2007) 1–6.
- [26] S.H. Lin, C.L. Lai, Catalytic oxidation of dye wastewater by metal oxide catalyst and granular activated carbon, *Environ. Int.* 25 (4) (1999) 497–504.